

A 550-GHZ DUAL POLARIZED QUASI-OPTICAL SIS MIXER

Goutam Chattopadhyay, David Miller, and Jonas Zmuidzinas

California Institute of Technology, 320-47, Pasadena, CA 91125, USA.

Henry G. LeDuc

Jet Propulsion Laboratory, 320-231, Pasadena, CA 91125, USA.

Abstract

We describe the design, fabrication, and the performance of a low-noise dual-polarized quasi-optical superconductor insulator superconductor (SIS) mixer at 550 GHz. The mixer utilizes a novel cross-slot antenna on a hyperhemispherical substrate lens, two junction tuning circuits, niobium trilayer junctions, and an IF circuit containing a lumped element 180° hybrid. The antenna consists of an orthogonal pair of twin-slot antennas, and has four feed points, two for each polarization. Each feed point is coupled to a two-junction SIS mixer, and therefore, for each polarization there are two IF outputs and four junctions, for a total of eight junctions on the chip. Due to the mixer structure and the use of series bias of the junction pairs, it turns out that the two IF outputs for a given polarization are 180° out of phase, requiring a 180° hybrid to combine the IF outputs. The hybrid is implemented using a combination of lumped element/microstrip circuit located inside the mixer block. Fourier transform spectrometer (FTS) measurements of the mixer frequency response show good agreement with computer simulations. The measured co-polarized and cross-polarized patterns for both polarizations also agree well with the theoretical predictions. The noise performance of the dual polarized mixer is excellent, giving uncorrected receiver noise temperature of better than 115K (DSB) at 528 GHz for both the polarizations.

I. INTRODUCTION

Dramatic advances in millimeter and submillimeter wave receivers in recent years have resulted from the development of sensitive superconductor insulator superconductor (SIS) mixers, which now offer unsurpassed performance from 70 GHz to 1 THz. In principle, the sensitivity of SIS mixers is limited only by the zero-point quantum fluctuations of the electro-magnetic field. In terms of the single-sideband (SSB) noise temperature, this limit is $h\nu/k_B \approx 0.05$ K/GHz. In practice, the SSB noise temperatures of the best SIS receivers now fall below 0.5 K/GHz over the 100-700 GHz band, dropping as low as 0.2 K/GHz in some cases. One should note that 0.5 K/GHz is about the level of performance of HEMT amplifiers in the 30 GHz band. SIS mixers have improved to the point that optical elements such as the cryostat vacuum window and the LO injection beamsplitter often contribute a significant fraction of the receiver noise.

One way to increase the sensitivity of SIS receivers further is to use a dual polarized receiver. When both polarizations are received simultaneously, there is a $\sqrt{2}$ improvement in signal to noise (S/N) or a factor of two reduction in observing time. Dual polarization operation can be achieved by using a wire grid polarizer to split the telescope beam into two polarizations. The local oscillator (LO) can be injected using a beamsplitter, either

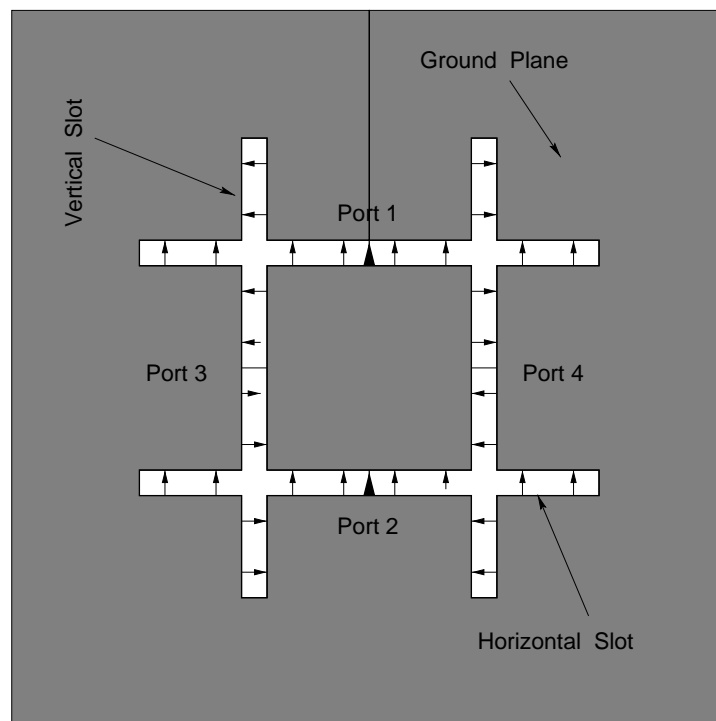


Fig. 1. Cross-slot antenna structure showing the field distribution in the slots when the two horizontal slots are excited symmetrically.

after the polarizer, in which case two beamsplitters are necessary; or before the polarizer, necessitating a single, correctly oriented beamsplitter. Either approach tends to lead to fairly complicated optical designs, especially for receivers with multiple bands. A much more elegant and compact solution is to directly construct a dual-polarization mixer. This is reasonably straightforward for quasi-optical designs, since the receiving antenna is lithographically fabricated, and can be designed to receive both polarizations simultaneously. The slot-ring mixer is one such example where a single annular (circular or square-shaped) slot is used, which is fed at two points which are 90° apart, and which has been shown to provide good results at 94 GHz [1]. A slot-ring antenna could easily be adapted for use in a SIS mixer. One drawback for this antenna is that it has a broader radiation pattern (in angle) than the twin-slot antenna [2]. This is simply due to the fact that at any given frequency, the transverse dimensions of a slot-ring are smaller than those of a twin-slot. This broader pattern of the slot-ring will be somewhat more difficult to couple to, so the efficiency will be a bit lower than for a twin-slot.

However, we adapted the twin-slot antenna for dual-polarization simply by crossing two sets of slots at 90° , as shown in Fig. 1. In this case, there are four feed points as can be seen in the figure. The field distribution in the slots can be intuitively obtained from symmetry considerations. In particular, the field distributions in the vertical slots must be antisymmetric and, therefore, the voltage at the orthogonal ports (3,4) must vanish. The characteristics of the cross-slot antenna have been calculated using the method of moments

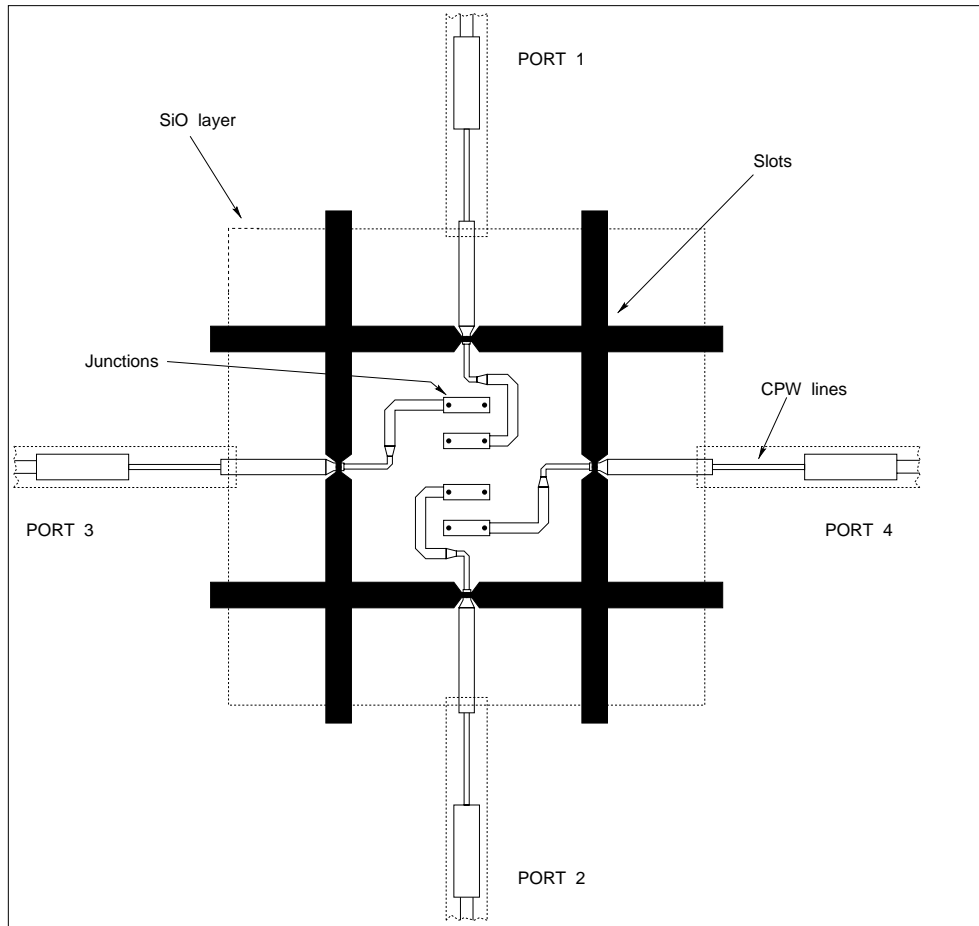


Fig. 2. Details of the mixer layout. CPW lines carry the IF output to the 180° hybrid. The junctions are placed as shown to allow suppression of the Josephson effect with a single magnet.

(MoM), and this design was found to have an excellent radiation pattern with fairly symmetric E-plane and H-plane beams, low impedance, wide bandwidth, low cross polarization, and high coupling efficiency [3].

II. MIXER DESIGN AND FABRICATION

To design an SIS mixer using the crossed-slot antenna, the easiest method would be to couple a separate tuned SIS circuit to each of the four ports. One possible concern in this approach would be that the resonant frequencies of the four SIS circuits might not all be the same, which would lead to degraded cross-polarization, and inferior performance overall. To minimize this effect, we decided to use tuning circuits in which the junction *separation* dictates the tuning inductance. The four SIS circuits are combined into the two horizontal and vertical polarization outputs simply by biasing in series from IF port 1 to 2, and from 3 to 4. This also eliminates the necessity of attaching an electrical connection to the isolated

ground plane in the center of the cross-slot. Fig. 2 shows the details of the mixer layout. The mixer tuning circuit design is quite similar to twin-slot mixer described by Zmuidzinas *et al.* [5]. The two section microstrip transformer, shown in Fig. 2, allows a good impedance match between the antenna ($\approx 30 \Omega$) and the tunnel junctions ($\approx 7 \Omega$). The relatively low antenna impedance promotes good matching to even low resistance tunnel junctions. We used a simulation program, developed in house [6], to simulate and optimize the RF device performance. We used JPL's all optical-lithography junction fabrication process to fabricate junctions with three different junction areas $1.44 \mu\text{m}^2$, $1.69 \mu\text{m}^2$, and $1.96 \mu\text{m}^2$. Though the design was optimized for $1.69 \mu\text{m}^2$ area junctions, we decided to fabricate three different junction area devices to allow for process variations. We used a three mask level Nb/Al-Oxide/Nb junction fabrication with a 2000 \AA thick niobium ground plane, 2500 \AA thick niobium wiring layer and a single layer of 2000 \AA thick SiO which is used as the dielectric for the superconducting microstrip line. The SIS mixer chip is placed on a hyperhemispherical silicon substrate lens. It can be seen from Fig. 2 that for each polarization there are two IF outputs and four SIS junctions, for a total of eight junctions on the chip. In principle, single junction mixers could also be used, which would require only four junctions per chip.

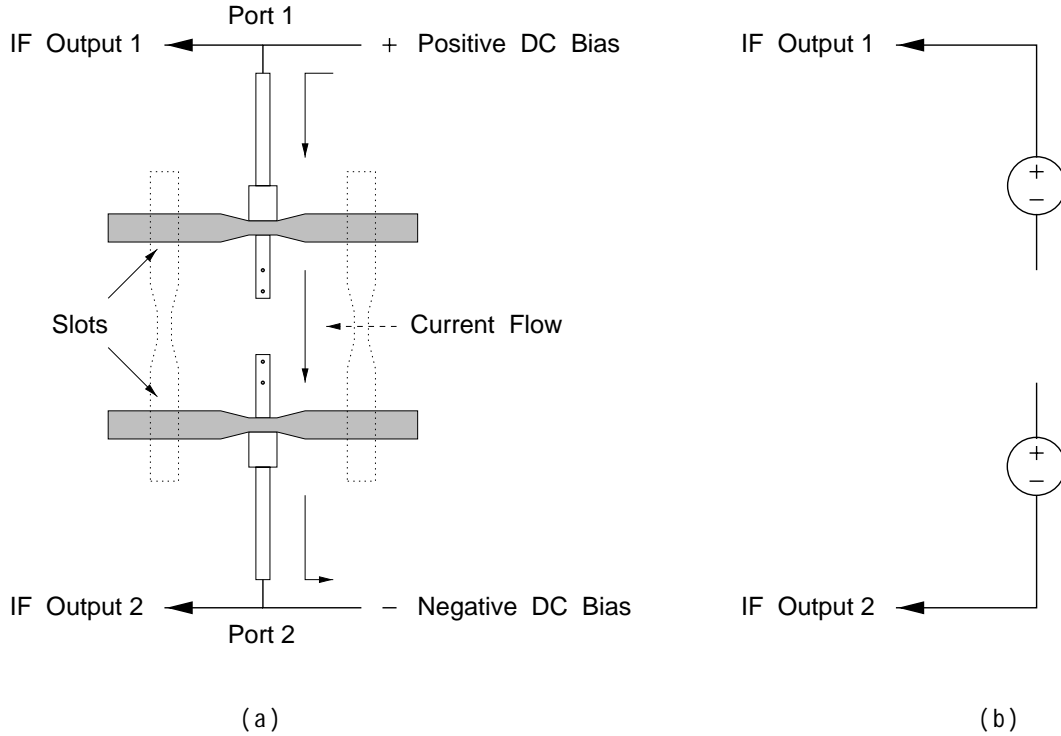


Fig. 3. Schematic showing how the two IF outputs for a given polarization are 180° out of phase : (a) shows the current flow for biasing the junctions in series and (b) shows the equivalent circuit.

Due to the mixer structure and the series bias of the junction pairs, it turns out that the two IF outputs for a given polarization are 180° out of phase. This can be easily explained. For a given polarization (let's assume for the horizontal pair of slots), the LO and RF will

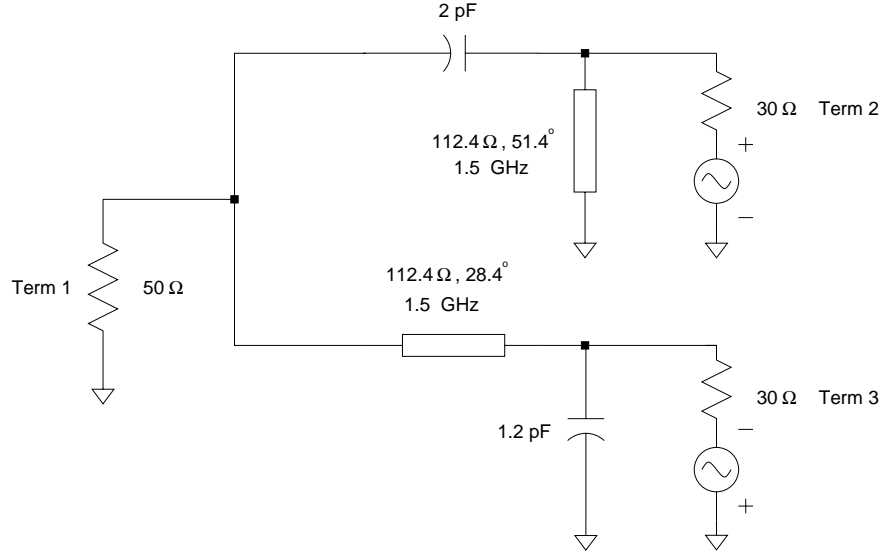


Fig. 4. Circuit diagram for the 180° hybrid.

have the same relative phase at either port (1 or 2), so we would expect the IF currents to be in phase. However, due to the series biasing of the junctions one junction pair is “forward” biased while the other is “reverse” biased. As shown in the equivalent circuit in Fig. 3(b), the two IF outputs are 180° out of phase and hence, a 180° hybrid is necessary to combine the IF outputs. The hybrid circuit is designed using a first order lowpass-highpass filter combination, whose bandwidth at 1.5 GHz center frequency is wide enough for our 500 MHz bandwidth HEMT amplifier. The hybrid is implemented using a combination of lumped element/microstrip circuit as shown in Fig. 4, and is located inside the mixer block. The circuit was optimized using Hewlett Packard’s microwave design system (MDS) [7] to deliver maximum power to a 50 Ω load at terminal 1 (the LNA input impedance) from two 180° out of phase 30 Ω generators at terminals 2 and 3 (the SIS IF output impedance). We have measured the input reflection coefficient (S_{11}) of the lumped hybrid IF circuit at cryogenic temperatures to evaluate its performance and to verify the design.

III. RECEIVER CONFIGURATION

A general view of the receiver configuration is shown in Fig. 5, specific modifications for single and dual-polarization measurements will follow in the next section. The LO used is a tunable Gunn oscillator with a varactor multiplier [8], [9]. The RF signal and the LO inputs pass through a 10 μm thick mylar beamsplitter and the combined signal travel into the cryostat through a 3.8 mm thick crystal quartz pressure window at room temperature, followed by a 0.1 mm thick Zitex [10] IR filter at 77 K. Inside the cryostat the well-collimated ($\approx F/17$) beam is matched to the broad beam pattern of the cross-slot antenna with a polyethylene lens and a silicon hyperhemisphere lens with anti-reflection (AR) coating of alumina-loaded epoxy [5], [11]. The quartz pressure window is AR coated with Teflon.

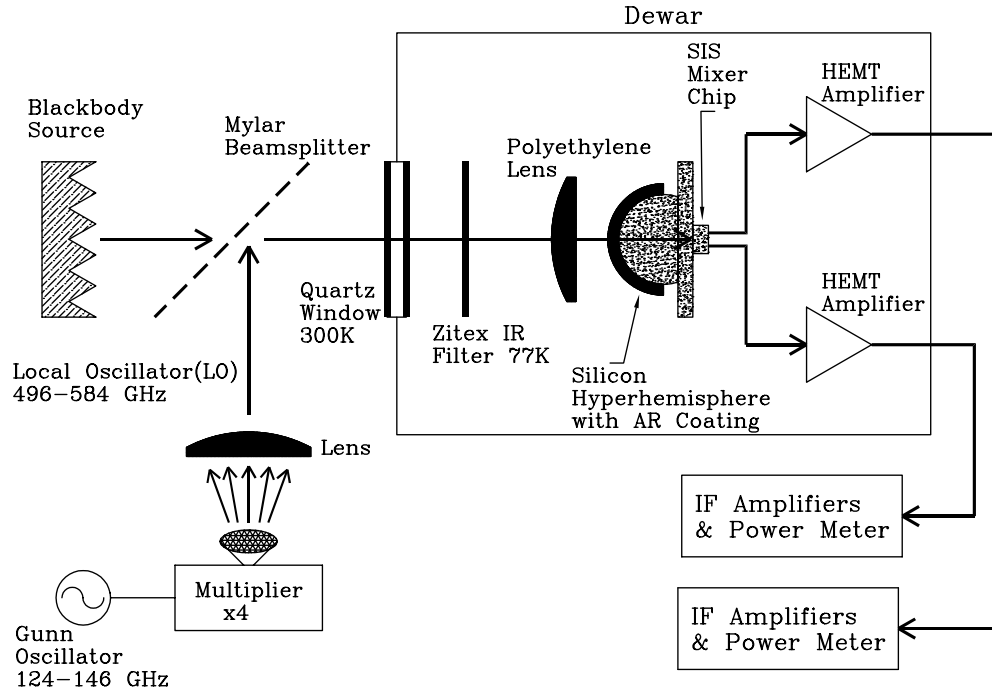


Fig. 5. Simplified receiver layout. The elements within the dewar are mounted on a 4.2 K cold plate.

For the dual-polarization mixer, we used our existing single polarization mixer block, described in detail by Gaidis *et al.* [12], with some minor modifications, such as another SMA connector to bring out two IF outputs for the two polarizations. Fig. 6 presents a detailed view of the mixer block and the associated circuitry. Fig. 6(a) shows a disassembled block with the mixer chip at the center. Fig. 6(b) shows the hardware details for the mixer block and Fig. 6(c) shows the bias and IF circuitry. The back side of the SIS mixer chip is glued [13] to one side of a silicon support disk, and the silicon hyperhemisphere is glued [13] to the opposite side of the disk. The SIS devices are fabricated on a 0.25 mm thick, 50 mm diameter silicon wafer, which is then diced into 2.0 x 2.0 mm individual chips. The high resistivity ($> 1000 \Omega\text{-cm}$) silicon support disk is 2.5 cm in diameter and 1.0 mm thick. The silicon hyperhemisphere is similar to the one described by Gaidis *et al.* [12].

The silicon disk is clamped in the mixer block by a printed circuit board, which itself is held in place by metal clamps and screws as shown in Fig. 6(a). The circuit board is 0.64 mm thick TMM6 temperature stable microwave laminate from Rogers corporation [14], with room temperature dielectric constant 6.0.

DC bias supply and readout leads enter from the multi-pin connector on the right, and the mixer outputs, after being combined by the 180° hybrids, are carried on two different microstrip lines to SMA connectors on the left. The schematic in Fig. 6(c) details the circuitry on the printed circuit board. The dc bias source resistance is adjustable by feedback to present the mixer with either a current source or a voltage source. Resistor R_{neg} is chosen at approximately 100Ω to prevent unstable biasing due to regions of negative dynamic resis-

tance in the SIS I-V curve. The current-sensing resistor R_{sense} is $10\ \Omega$, and the IF-blocking spiral inductors ($17\ \text{nH}$) at liquid helium temperature ($4.2\ \text{K}$) add $\ll 1\ \Omega$ series resistance. The $150\ \text{pF}$ dc blocking capacitors in Fig. 6(c) are attached to the IF output microstrips with silver-loaded epoxy. The chip inductors are wire-bonded to the top electrodes of the $150\ \text{pF}$ bypass capacitors. The SIS mixer chip sits within a through hole at the center of the board, allowing straight forward wire-bonding of the mixer chip to the biasing network and to the 180° hybrid circuits. The remaining chip resistors, chip capacitors, and connector pins are attached to the circuit board traces with either solder or silver-loaded epoxy.

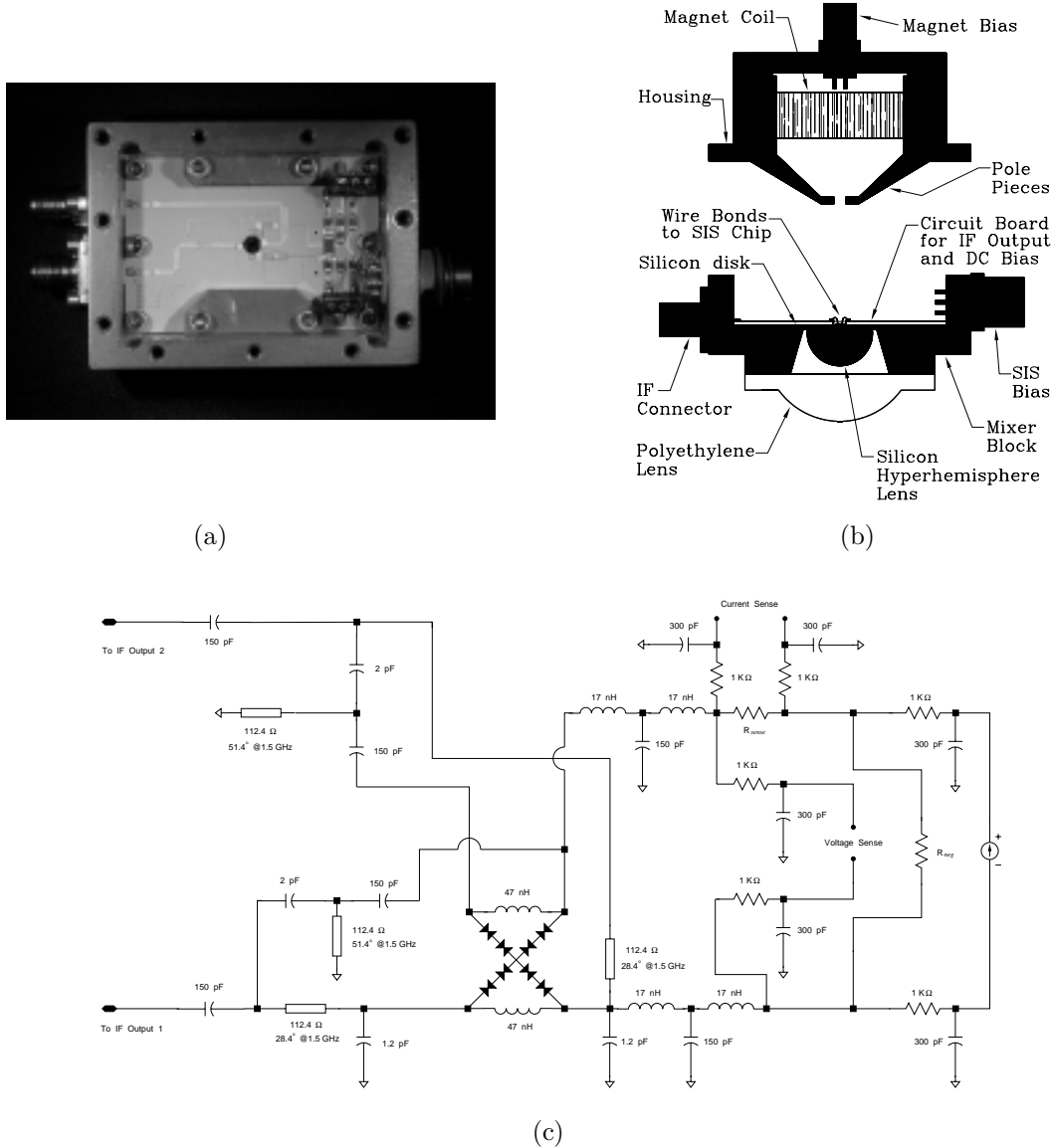


Fig. 6. Details of the mixer block and associated circuitry : (a) shows the block revealing the internal components, (b) provides a key to the hardware used within the block, (c) shows the details of biasing circuit along with the components on the printed circuit board.

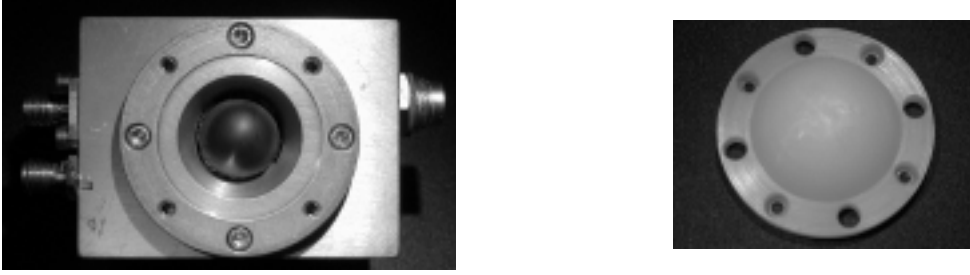


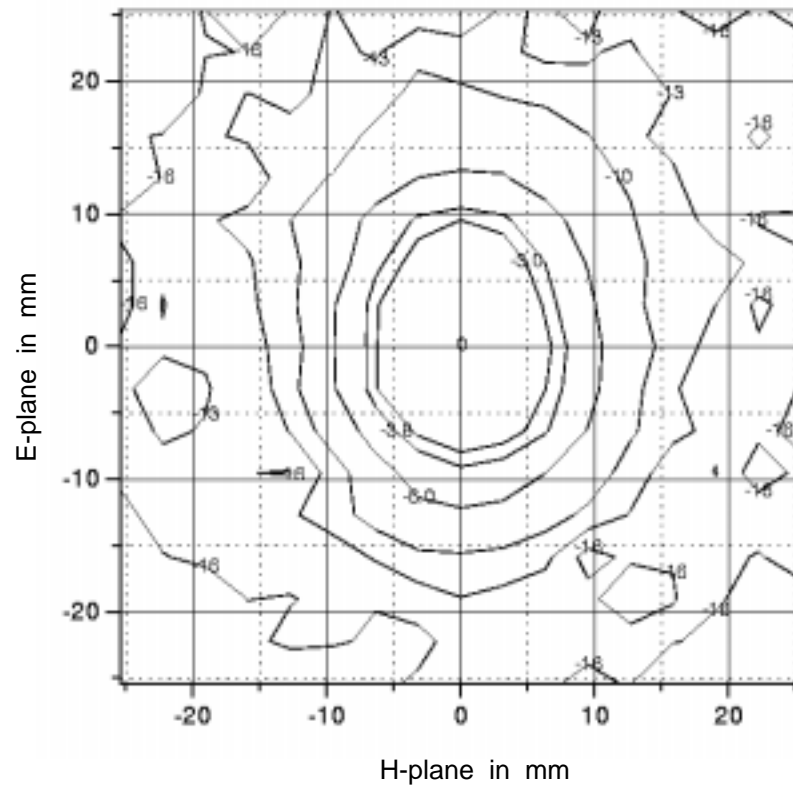
Fig. 7. Actual picture of an assembled block, with the polyethylene lens removed to show the AR coated silicon hyperhemisphere.

The picture in Fig. 7 shows the assembled mixer block, with the polyethylene lens removed to reveal the silicon hyperhemispherical lens. Semi-rigid coaxial cables connect the SMA ports with HEMT low noise amplifiers (LNAs). The measurements presented below were obtained using a 1.0-2.0 GHz LNA with measured noise temperatures of 5 K [15]. The LNA outputs are sent to room temperature amplifiers and diode detectors which measure the total power in 500 MHz IF bandwidth.

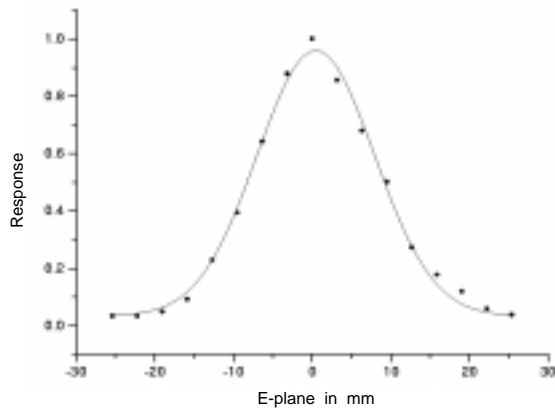
IV. MEASUREMENT AND RESULTS

A. Antenna Beam Pattern Measurements

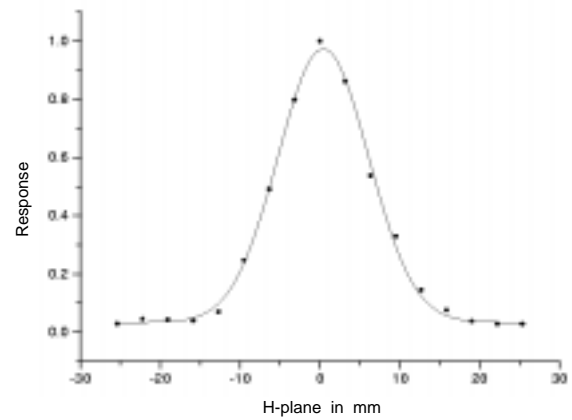
The beam pattern of the dual polarized antenna was measured with an antenna measurement system built in-house [16]. The test setup consists of an aperture limited chopped hot-cold load on a x-z linear stage, stepper motors to drive the linear stage, a lock-in amplifier, and a data acquisition system. The IF output of the mixer is detected and amplified in a total power box and is fed in to the lock-in amplifier. The hot-cold load linear stage was placed at 24 cm away from the cryostat vacuum window for our beam pattern measurement. The hot-cold load aperture was set at 3.2 mm and the lock-in amplifier time constant was set at 3 seconds, giving signal to noise of about 18 dB for the measurement set-up. The mixer was pumped with a 528 GHz LO source. The hot-cold RF signal and the LO were coupled to the junction through a 10 μ m thick beamsplitter. Fig. 8 shows the co-polarized beam pattern along with E-plane and H-plane cuts for the horizontal pair of slots and Fig. 9 shows the same for the vertical pair of slots. The E-plane beam is wider than the H-plane beam (as is expected) for both the polarizations. For the horizontal slots, the E-plane and H-plane FWHM was found to be 18.5 mm and 14 mm respectively, giving E/H ratio of 1.3, which is higher than our theoretical prediction of 1.1. The discrepancy between the measured and the calculated beam asymmetry may be a result of distortion of the shape of the plastic lens at liquid helium temperature (4.2 K). We are currently investigating this possibility. Similarly, for the vertical slots, the E-plane and H-plane FWHM was found to be 18 mm and 13 mm respectively. For cross polarization measurement we used a wire grid polarizer in front of the cryostat window. The hot-cold load aperture was set at 6.4 mm and the lock-in amplifier time constant was set at 10 seconds, which improved the signal to noise to about 28 dB. The cross polarization beam pattern is shown in Fig. 10. It can be seen from the cross polarization beam pattern that the cross polarization is indeed low as predicted by MoM calculations [3].



(a)

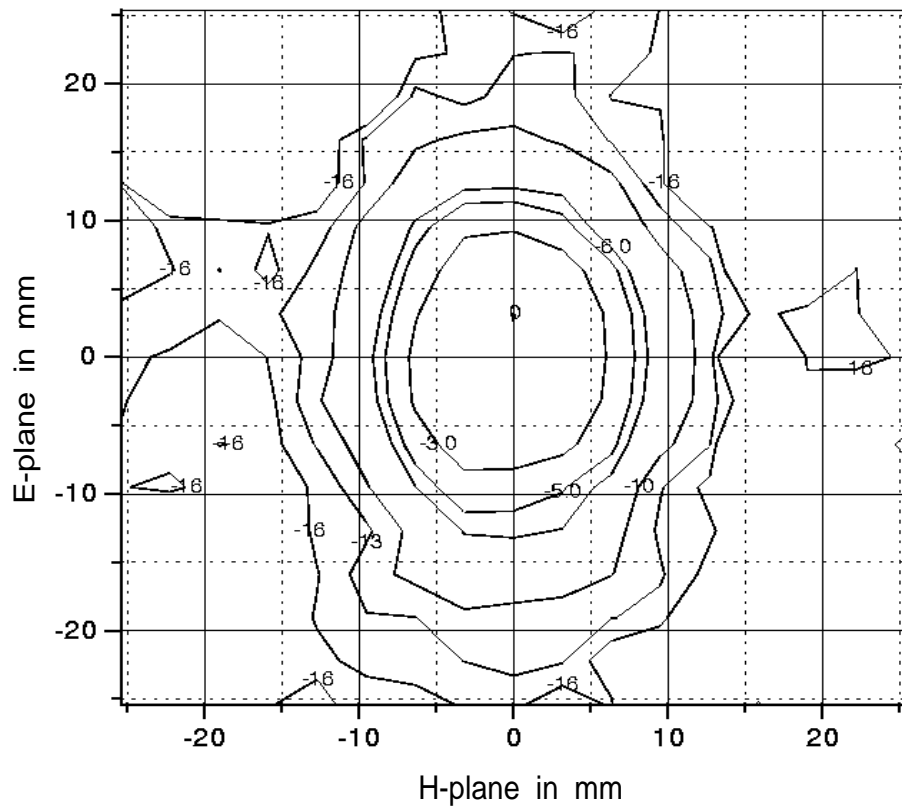


(b)

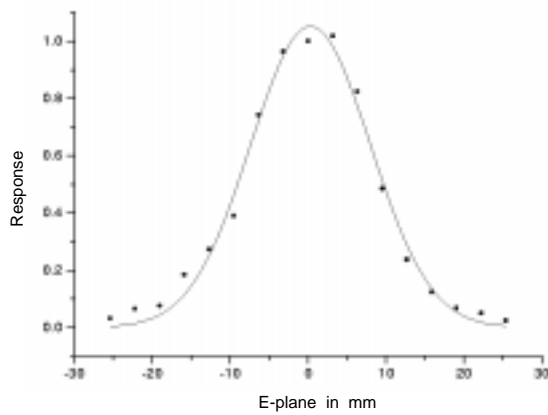


(c)

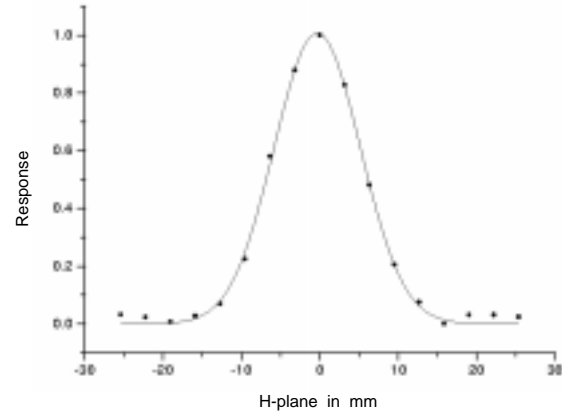
Fig. 8. Antenna beam pattern for the horizontal pair of slots : (a) shows the contour plot, (b) and (c) are the E-plane and H-plane cuts for the beam. The LO frequency for the beam pattern measurement was set at 528 GHz.



(a)



(b)



(c)

Fig. 9. Antenna beam pattern for the vertical pair of slots : (a) shows the contour plot, (b) and (c) are the E-plane and H-plane cuts for the beam. The LO frequency for the beam pattern measurement was set at 528 GHz.

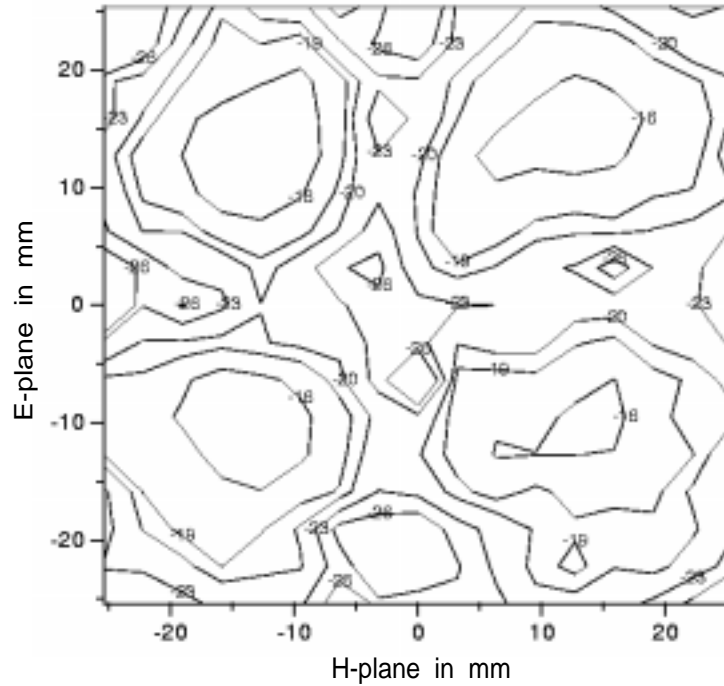


Fig. 10. Cross-polarization beam pattern in dB relative to peak co-polarized power. The LO frequency for the beam pattern measurement was set at 528 GHz.

B. Fourier Transform Spectroscopy

The receiver response as a function of frequency was measured with an FTS system built in-house using the mixer as a direct detector [17]. Although we can not measure the *absolute* response using the FTS, the *shape* of the relative response as a function of frequency is quite reliable and useful. Fig. 11 shows the FTS response for each polarization of the receiver. The device we used for this measurement was a $1.69 \mu\text{m}^2$ area junction optimized for 550 GHz frequency band. The FTS response agrees well with our simulation results, as can be seen from Fig. 11. The dip around 550 GHz is due to the water absorption line, shown by the transmission graph. The FTS response is very similar for both the polarizations, and the peak response was found at 528 GHz, which means that the best noise temperature should be around that frequency.

C. Heterodyne Measurements

We measured the noise temperature of the receiver, for both the polarizations, first with one polarization active at a time, and then with both polarizations simultaneously active, using the Y-factor method. The cryostat temperature was 4.2 K for all the measurements. The noise temperatures reported here are referred to the input of the beamsplitter; *no corrections have been made for beamsplitter or any other optical losses.*

For measuring one polarization at a time, we mounted the device in such a way that the active pair of slots was horizontal with respect to Fig. 6(a) and biased only two of the ports

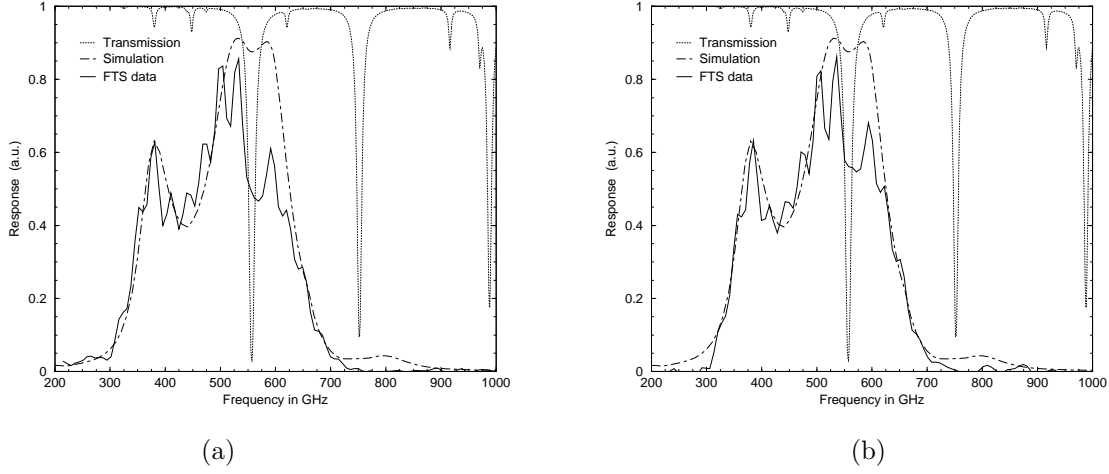


Fig. 11. FTS measured response (solid lines) versus mixer simulation (dashed lines) : (a) for the horizontal slots and (b) for the vertical slots. The dotted lines show the transmission for the instrument.

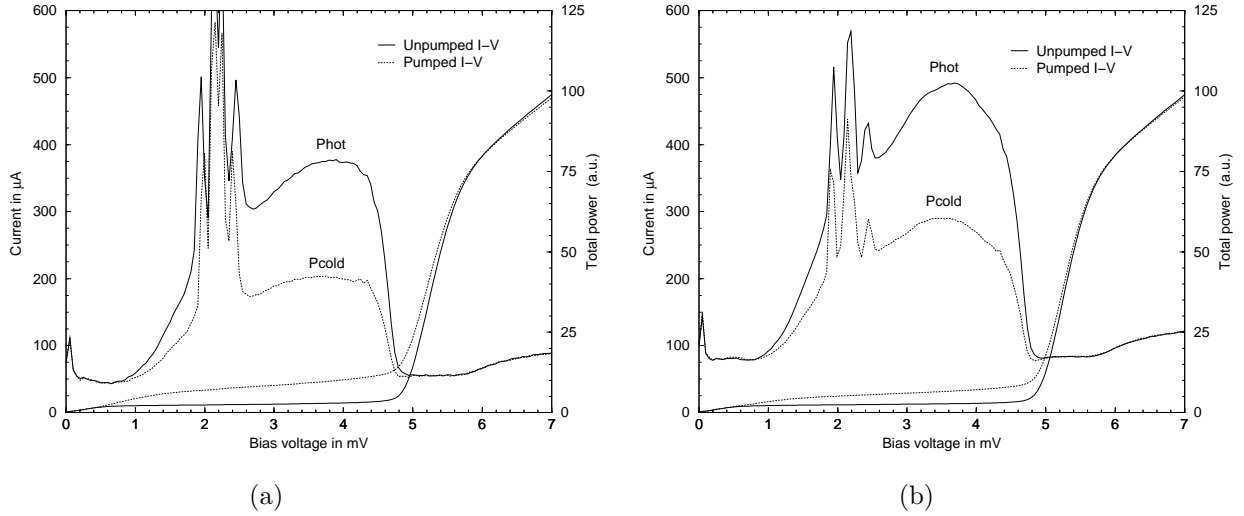


Fig. 12. Current and IF power versus bias voltage at 4.2 K : (a) for the horizontal polarization and (b) for the vertical polarization. The LO frequency for both of them is 528 GHz and the measured DSB receiver noise temperatures are 145 K.

at a time (1,2 or 3,4) in series. The correctly polarized LO pumped only four junctions for the active polarization. Fig. 12 shows the d-c current voltage characteristics for the “horizontal” and the “vertical” pair of slots. The pumped and unpumped I-V curves clearly show the photon step around $V \approx 1.4$ mV, as expected from a 528 GHz LO source ($h\nu/e \approx 2.2$ mV, since the junctions are in series, the gap voltage is at 5.8 mV and the photon step will appear at $5.8 \text{ mV} - 2 \times 2.2 \text{ mV} = 1.4 \text{ mV}$). Also shown in Fig. 12 are the total IF output power in a 500 MHz bandwidth when hot and cold loads (absorber at room temperature and at 80 K respectively) are placed at the receiver input. The curves for both the polarizations are relatively smooth, in spite of the fact that four junctions were under a single magnet,

indicating good suppression of Josephson noise. At 528 GHz the best DSB noise temperature was measured to be 145 K for both the polarizations. We also measured noise temperatures at frequencies from 512 GHz to 580 GHz, and found that the results closely follow the FTS response, giving close to the best noise temperature near 528 GHz, getting worse near the water absorption line and getting better again towards the 570 GHz range.

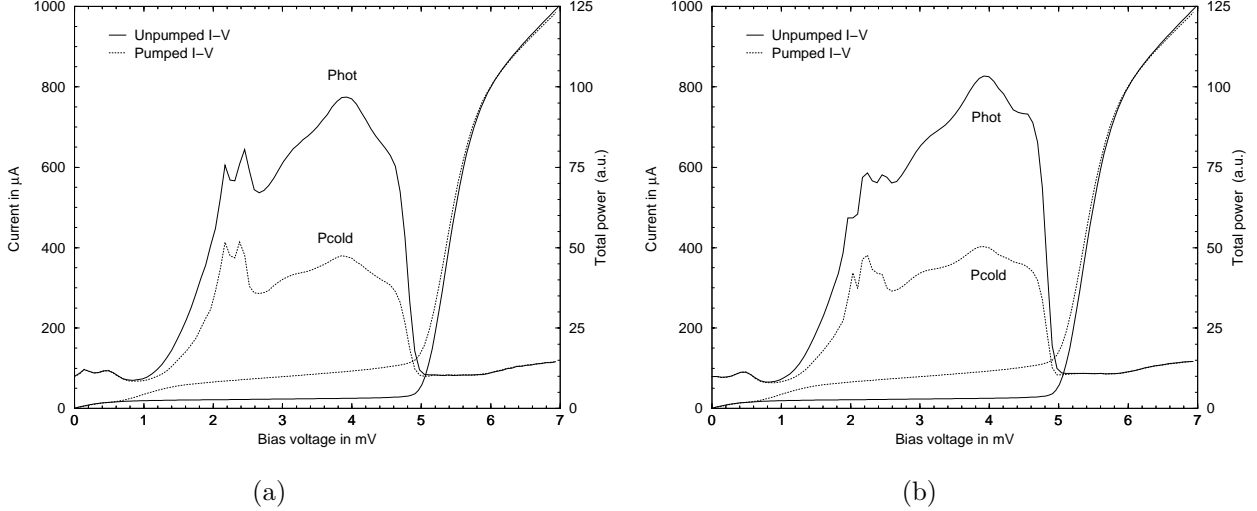


Fig. 13. Current and IF power versus bias voltage at 4.2 K when we measured both the polarizations simultaneously : (a) for the “horizontal” polarization and (b) for the “vertical” polarization. The LO frequency for both of them is 528 GHz and the measured DSB receiver noise temperatures are 115 K.

For measuring noise temperature for both the polarizations at once, we mounted the device at 45° angle with respect to the horizontal microstrip line shown in Fig. 6(a). The junctions are biased as shown in Fig. 6(c), where the IF outputs of the two different polarizations are isolated from each other by two 45 nH spiral inductors. A single LO source pumped the junctions for both the polarizations simultaneously. We confirmed that we indeed were measuring two orthogonal polarizations at the same time by using a wire grid polarizer in between a cold load (80 K) and the beamsplitter input. As we rotated the wire-grid, the cold load became visible to one polarization and its IF output power went down while the IF output power for the other polarization went up as it could not see the cold load, confirming dual-polarization operation. We adjusted the LO and the magnet current to get a smooth IF output for both the polarizations and then measured the noise temperature. Fig. 13 shows the pumped and the unpumped I-V curves along with the IF outputs for hot and cold loads at 528 GHz. We measured DSB noise temperature of 115 K for both the polarizations at 528 GHz. The receiver noise temperature was also measured from 512 GHz to 580 GHz range and was found to be similar to the single polarization measurement.

V. CONCLUSION

We have designed, fabricated and measured a dual-polarized quasi-optical SIS receiver at 550 GHz using a cross-slot antenna structure on a anti-reflection coated hyperhemispherical silicon lens which gives excellent noise temperature performance (115 K DSB) for both the polarizations. The measured antenna radiation patterns agree reasonably well with theoretical predictions. We have shown that this receiver has almost identical performance for both the polarizations, and could be very effectively used for submillimeter radio astronomy observations. We think the improvement in the performance of the receiver would be possible if we integrate the 180° hybrid with the SIS chip. It is also possible to use this device as a balanced mixer and we will look into that in future.

ACKNOWLEDGMENTS

This work was supported in part by NASA/JPL and its Center for Space Microelectronics Technology, by NASA grants NAG5-4890, NAGW-107, and NAG2-1068, by the NASA/USRA SOFIA instrument development program, and by the Caltech Submillimeter Observatory (NSF grant AST-9615025).

REFERENCES

- [1] S. Raman, and G. M. Rebeiz, "Single- and dual-polarized millimeter-wave slot-ring antennas," *IEEE Trans. Antennas Propagat.*, vol. AP-44, no. 11, pp. 1438-1444, November 1996.
- [2] J. Zmuidzinas, and H. G. LeDuc, "Quasi-optical slot antenna SIS mixers," *IEEE Trans. Microwave Theory Tech.*, vol. MTT-40, no. 9, pp. 1797-1804, September 1992.
- [3] G. Chattopadhyay, J. Zmuidzinas, "A dual-polarized slot antenna for millimeter waves," *IEEE Trans. Antennas Propagat.*, vol. AP-46, no. 5, pp. 736-737, May 1998.
- [4] J. Zmuidzinas, H. G. LeDuc, J. A. Stern, and S. R. Cypher, "Two-junction tuning circuits for submillimeter SIS mixers," *IEEE Trans. Microwave Theory Tech.*, vol. MTT-42, no. 4, pp. 698-706, April 1994.
- [5] J. Zmuidzinas, N. G. Ugras, D. Miller, M. C. Gaidis, H. G. LeDuc, and J. A. Stern, "Low-noise slot antenna SIS mixers," *IEEE Trans. Appl. Superconduct.*, vol. 5, pp. 3053-3056, 1995.
- [6] M. Bin, "Low-noise THz Niobium SIS mixers," PhD Dissertation, California Institute of Technology, Pasadena, October 1996.
- [7] Microwave Design Systems (MDS) version mds.07.10, Hewlett Packard Company, Test and Measurement Organization, Palo Alto, CA.
- [8] J. E. Carlstrom, R. L. Plembeck, and D. D. Thornton, "A continuously tunable 65-115 GHz Gunn oscillator," *IEEE Trans. Microwave Theory Tech.*, vol. MTT-33, no. 7, pp. 610-619, July 1985.
- [9] N. R. Erickson, "High efficiency submillimeter frequency multipliers," *1990 IEEE MTT-S Int'l Microwave Symp.*, pp. 1301, June 1990.
- [10] *Zitex* - Norton Co. Wayne, NJ 201696-4700.
- [11] Janos Technology, Inc., HCR #33, Box 25, Route 35, Townshend, VT 05353-7702.
- [12] M. C. Gaidis, H. G. LeDuc, M. Bin, D. Miller, J. A. Stern, and J. Zmuidzinas, "Characterization of low-noise quasi-optical SIS mixers for the submillimeter band," *IEEE Trans. Microwave Theory Tech.*, vol. MTT-44, no. 7, pp. 1130-1139, July 1996.
- [13] Litetak 3761 UV-curing adhesive, by Loctite Corp., Hartford, CT 06106.
- [14] Rogers Corporation, Microwave Circuit Materials Division, 100 S. Roosevelt Ave., Chandler, AZ 85226.
- [15] J. W. Kooi, California Institute of Technology, Pasadena, CA, *private communications*.
- [16] David A. Miller, "Comparison between theory and measurement of beam patterns for double-slot quasi-optical SIS mixers," MSEE Dissertation, California State Polytechnic University, Pomona, May 1998.
- [17] Q. Hu, C. A. Mears, P. L. Richards, and F. L. Lloyd, "Measurement of integrated tuning elements for SIS mixers," *Int. J. IR and MM Waves.*, vol. 9, pp. 303-320, 1988.